Effect of Depolarization on Binding Kinetics of Scorpion α-Toxin Highlights Conformational Changes of Rat Brain Sodium Channels[†]

Nicolas Gilles,[‡] Enrico Leipold,[§] Haijun Chen,[§] Stefan H. Heinemann,[§] and Dalia Gordon*[,||]

Commissaariat à l'Energie Atomique, Département d'Ingénierie et d'Etudes des Protéines, Centre d'Etudes de Saclay, 91191 Gif-sur-Yvette, France, Molecular and Cellular Biophysics, Medical Faculty of the Friedrich Schiller University Jena, Drackendorfer Strasse 1, D-07747 Jena, Germany, and Department of Plant Sciences, Tel-Aviv University, Ramat-Aviv, Tel Aviv, 69978 Israel, and Sigyn Pharmaceuticals Ltd., Post Office Box 45010 Jerusalem, 91450 Israel

ABSTRACT: Binding of scorpion α-toxins to receptor site 3 on voltage-gated sodium channels inhibits sodium current inactivation and is voltage-dependent. To reveal the direct effect of depolarization, we analyzed binding kinetics of the α-toxin Lqh-II (from *Leiurus quinquestriatus hebraeus*) to rat brain synaptosomes and effects on rat brain II (rBII) channels expressed in mammalian cells. Our results indicated that the 33-fold decrease in toxin affinity for depolarized (0 mV, 90 mM $[K^+]_{out}$, $K_d = 5.85 \pm 0.5$ nM) versus polarized (-55 mV, 5 mM $[K^+]_{out}$, $K_d = 0.18 \pm 0.04$ nM) synaptosomes at steady state results from a 48-fold reduction in the association rate (k_{on} at 5 mM $[K^+] = (12.0 \pm 4) \times 10^6$ M^{-1} s^{-1} and $(0.25 \pm 0.03) \times 10^6$ M^{-1} s^{-1} at 90 mM $[K^+]_{out}$) with nearly no change in the dissociation rate. Electrophysiological analyses of rBII channels expressed in mammalian cells revealed that approximately 75% and 40% of rBII occupied fast- and slow-inactivated states, respectively, at resting membrane potential of synaptosomes (-55 mV), and Lqh-II markedly increased the steady-state fast and slow inactivation. To mimic electrophysiological conditions we induced fast depolarization of toxin-bound synaptosomes, which generated a biphasic unbinding of Lqh-II from toxin−receptor complexes. The first fast off rate closely resembled values determined electrophysiologically for rBII in mammalian cells. The second off rate was similar to the voltage-independent steady-state value, attributed to binding to the slow-inactivated channel states. Thus, the Lqh-II voltage-dependent affinity highlights two independent mechanisms representing conformational changes of sodium channels associated with transitions among electrically visible and invisible inactivated states.

Voltage-gated sodium channels (Na$^+$ channels) are responsible for the generation and propagation of action potentials in most excitable cells. These channels are composed of a pore-forming α-subunit, which contains four domains consisting each of six transmembrane segments (*1*). The fourth transmembrane segment (S4) in each domain contains several positive charges and serves as the voltage sensor of the channel (*2*, *3*). The outward movements of S4 segments initiates the voltage-dependent activation of the Na$^+$ channel under membrane depolarization (*2*, *4*, *5*), with S4 of domain IV preceding the movement of the others (*6*). Domain IV prevails in the fast inactivation of Na$^+$ channels (*6−12*), a process that involves also the intracellular linker between domains III and IV (*2*, *13*, *14*).

Many neurotoxins bind to Na$^+$ channels at several receptor sites and affect the Na$^+$ current in various fashions (*15− 17*). Toxins that target Na$^+$ channel receptor site 3 bind in a voltage-dependent manner and inhibit the fast inactivation process (*15*, *16*, *18*). Receptor site 3 involves external regions of channel domains I and IV (*19*, *20*). A negatively charged amino acid residue at the external loop connecting segments S3 and S4 in domain IV has been shown to be very important for binding of site 3 toxins (*21−23*). In turn, the bioactive surface of site 3 toxins contains positively charged residues (*22*, *24*, *25*). Binding of scorpion α-toxins has been useful in probing subtle conformational changes at the channel surface that occur during voltage-dependent gating as well as during modulation provoked by other groups of neurotoxins (*15*, *16*, *26−29*). However, the structural basis of the voltage dependency in binding of site 3 toxins and the mechanism by which binding to channel external regions affects fast inactivation, which is presumably mediated by intracellular protein components, is still elusive.

Depolarization of the membrane induces a dramatic decrease of the scorpion α-toxin affinity to Na$^+$ channels, as has been demonstrated in both electrophysiological and binding studies (*21*, *26*, *30−36*). The voltage-dependent drop in binding affinity has been attributed to an increase in the dissociation rate constant of α-toxins under depolarized conditions (*21*, *30−32*, *35−37*). The voltage dependence of the apparent binding correlates well with the voltage dependence of channel activation and the coupled fast

* Corresponding author: Department of Plant Sciences, Tel-Aviv University, Ramat-Aviv, Tel Aviv 69978, Israel. E-mail dgordon@ post.tau.ac.il; fax +972-3-640-6100; phone +972-3-640-9844.
[‡] CEA, Département d'Ingénierie et d'Etudes des Protéines, C.E. Saclay.
[§] Medical Faculty of the Friedrich Schiller University Jena.
[||] Tel-Aviv University and Sigyn Pharmaceuticals Ltd.

inactivation (*21, 26, 31*), suggesting that these conformational transitions weaken the toxin−channel interaction. However, the interactions of α-toxins with the electrically silent fast- and slow-inactivated channel states have not been described. Only experiments in which the physical binding of toxins to Na$^+$ channels are measured can infer about the binding properties of such states, but thus far, no detailed analysis of the binding kinetics to the different channel states at polarized and depolarized membrane potentials have been reported.

To study the direct effect of membrane depolarization on the interaction of a scorpion α-toxin with receptor site 3, we have undertaken a detailed kinetic analysis of the binding of Lqh-II,[1] a classical scorpion α-toxin highly active on mammals, from *Leiurus quinquestriatus hebraeus* (*38*), to rat brain synaptosomes. Lqh-II is highly similar in effects and binding properties to previously studied scorpion α-toxins (e.g., LqTx or Lqq-V from *Leiurus qinquestriatus qinquestriatus*, *15, 21, 26, 30−32*) and is almost identical in sequence to Aah-II, from *Androctonus australis hector* (*18, 29, 33, 38*). Synaptosomes are capable of retaining a resting membrane potential due to a passive K$^+$ efflux, which can be modulated in the range of −55 to 0 mV by changing the external K$^+$ concentration (*32, 33, 39−41*). In our binding studies we found, unexpectedly, that the dramatic reduction in Lqh-II binding affinity between −55 and 0 mV did not correspond with an increase in the dissociation rate constant (as previously concluded; *21, 26, 30, 31, 35*) but with a decrease in the association rate. The expected marked increase in the dissociation rate was obtained, however, under fast depolarization of synaptosomes. The physical binding experiments with synaptosomes were compared with electrophysiological data obtained for rBII Na$^+$ channels expressed in mammalian cells.

EXPERIMENTAL PROCEDURES

Materials. Scorpion toxin II from *Leiurus quinquestriatus hebraeus* was from Latoxan (20, Rue Leon Blum, 2600 Valance, France) and, in part, was a generous gift of Dr. Pierre Sautière (Institut Pasteur, Lille). Reverse-phase C$_{18}$ (250 × 4.6 mm; 300 Å, 5 μm particle size) HPLC column was from Vydac. Iodogen was from Pierce Chemical Co. (Rockford, IL). Carrier-free Na^{125}I was from Amersham (Buckinghamshire, U.K.). All other chemicals were of analytical grade. Filters for binding assays were GF/C glass fiber (Whatman, Maidstone, U.K.) preincubated in 0.3% polyethylenimine (Sigma, Steinheim, Germany).

Rat Brain Synaptosome Preparation. Rat brain synaptosomes were prepared from adult albino Sprague−Dawley rats (about 300 g, laboratory bred), according to the method described by Kanner (*42*). All buffers contained a mixture of proteinase inhibitors composed of phenylmethanesulfonyl fluoride (50 μg/mL), pepstatin A (1 μM), iodoacetamide (1 mM), and 1,10-phenanthroline (1 mM). All processes were performed on ice. The enriched synaptosomal fraction was frozen in aliquots at −80 °C. Membrane protein concentra-

tion was determined by Bio-Rad protein assay, with bovine serum albumin (BSA) as standard.

Radioiodination of Lqh-II. Lqh-II was radioiodinated by Iodogen (Pierce Chemical Co., Rockford, IL) with 5 μg of toxin and 0.5 mCi of carrier-free Na^{125}I, and the monoiodotoxin was purified on an analytical Vydac reverse-phase C$_{18}$ column, as was previously described (*43*). The concentration of the radiolabeled toxin was determined according to the specific activity of the ^{125}I, corresponding to 2500−3000 dpm/fmol of monoiodotoxin, depending on the age of the radiotoxin and by estimation of its biological activity (usually 60−70%; *44*).

Binding Assay. Rat brain synaptosomes were thawed at 37 °C (for 30 s) and placed on ice. The synaptosomes were suspended in 0.2 or 1 mL of binding buffer (13.6−78.8 μg of protein/mL), containing 33−268 pM ^{125}I-Lqh-II, depending on the type of experiment (see figure captions). After incubation for the designated time periods, the reaction mixture was diluted with 2 mL of ice-cold wash buffer and filtered through GF/C filters under vacuum. Filters were rapidly washed twice with 2 mL of wash buffer. Termination of reaction and washing lasted 10 s. Nonspecific binding of the toxin was determined in the presence of a high concentration of Lqh-II, as specified in the figure legends, and typically accounted for 5−30% of total binding of ^{125}I-Lqh-II. Standard binding medium composition (millimolar) was as follows: choline chloride 130, CaCl$_2$ 1.8, KCl 5, MgSO$_4$ 0.8, HEPES 50, glucose 10, and BSA 2 mg/mL. Wash buffer composition (millimolar) was as follows: choline chloride 140, CaCl$_2$ 1.8, KCl 5.4, MgSO$_4$ 0.8, HEPES 50 (pH 7.2), and BSA 5 mg/mL. When membranes were depolarized by high external K$^+$ concentration, choline chloride was substituted by KCl so that the total concentration of choline and K$^+$ was equal to 135 mM.

Equilibrium and Kinetic Analysis of Binding. Cold saturation assays were performed with increasing concentrations of unlabeled Lqh-II in the presence of a constant low concentration of ^{125}I-Lqh-II. The data were subjected to analysis by the iterative program LIGAND (Elsevier Biosoft, Cambridge, U.K.) by cold saturation analysis. The kinetic data for ligand association and dissociation rates were subjected to analysis by LIGAND, by kinetic analysis. Each curve was subjected to multislope analysis to detect the presence of one or two slopes. Toxin dissociation was induced by an excess of cold toxin and the dissociation rate constant (k_{off}) was determined directly from a first-order plot of toxin dissociation versus time. In some experiments (Figure 4), unbinding of toxin was determined by a time constant ($\tau = \ln 2/k_{off}$), estimated directly from the binding curves. The rate of toxin association (k_{on}) was determined from the equation $k_{on} = k_{obs}([RL]_e/([L][RL]_{max}))$, where [L] is the concentration of ligand, [RL]$_e$ is the concentration of the complex at equilibrium, [RL]$_{max}$ is the maximum number of receptors present (determined in a parallel saturation experiment), and k_{obs} is the slope of the pseudo-first-order plot ln {[RL]$_e$/([RL]$_e$ − [RL]$_t$)} versus time (*45*). Each experiment was performed at least three times and each data point represents the mean of 2−3 samples (with up to 12% deviation between samples). Data are presented as mean ± SEM of number (*n*) of independent experiments.

Expression of rBII Sodium Channels in Mammalian Cells. HEK293 or CHO cells were cultured according to standard

---

[1] Abbreviations: Lqh-II, α-toxin II from the scorpion *Leiurus quinquestriatus hebraeus*; HEPES, 4-(2-hydroxyethyl)-1-piperazineethanesulfonic acid; BSA, bovine serum albumin; K_d, dissociation constant; k_{on}, kinetic constant of association; k_{off}, kinetic constant of dissociation.

methods in a humid atmosphere incubator at 5% CO_2. Transient transfection of plasmid DNA was performed with the SuperFect transfection kit according to the manufacturer's description (Qiagen, Hilden, Germany). Cells grown to 30–50% confluence in 35-mm Petri dishes were cotransfected with a 5:1 ratio of Na^+ channel expression plasmid and a vector encoding the CD8 antigen (*46*). Plasmid DNA encoding Na^+ channels and the CD8 antigen was purified by Qiagen plasmid maxi kit (Qiagen). The coding segments of the rat brain II Na^+ channel, rBII (*1*), was cloned into the expression vector pCI-neo (Promega), kindly provided by Dr. K. Imoto (Okazaki, Japan). No difference in function of rBII channels was found between channels expressed in HEK293 or CHO cells.

Patch Clamp Recording. For patch clamp experiments, the cells were used 2–4 days after transfection. Before recording, transfected cells were incubated with Dynalbeads (Dynal GmbH, Hamburg, Germany) coated with antibodies directed against CD8 antigen for at least 30 min at 37 °C, in 5% CO_2, and washed a few times with the bath solution. Patch clamp experiments were performed with an EPC9 amplifier (HEKA Elektronik, Lambrecht, Germany). Data acquisition was controlled with Pulse+PulseFit software (HEKA Elektronik). The patch pipets were fabricated from borosilicate glass and had resistances of 0.8–2.0 MΩ when filled with internal solution (see below). They were coated with RTV 510 (General Electric) in order to reduce noise and electrical capacitance. Series resistances below 5 MΩ were accepted and a series resistance compensation of at least 80% was applied. Leak and capacitive transient currents were digitally subtracted online with procedures supported by the Pulse+PulseFit software. The holding voltage for all experiments was −120 mV.

Patch clamp pipets were filled with a solution containing (millimolar) NaCl 35, CsF 105, EGTA 10, and HEPES 10, pH 7.4. The bath solution contained (millimolar) NaCl 150, KCl 2, $CaCl_2$ 1.5, $MgCl_2$ 1, and HEPES 10, pH 7.4. The temperature was 20 ± 1 °C.

Lqh-II was dissolved in the bath solution, supplemented with 1 mg/mL BSA in order to prevent adherence of the toxin to the vials and the perfusion apparatus. The application of toxin was performed with an application pipet of about 10 μM opening diameter. The collection of the control data was initiated 15 min after the whole-cell voltage clamp configuration was established.

Further data analysis was performed with IgorPro software (WaveMetrics, Lake Oswego, OR). Steady-state inactivation was described with Boltzmann functions:

$$I/I_{max} = a_{ni} + (1 - a_{ni})/(1 + \exp[-(V - V_h)/k_h]) \quad (1)$$

with the voltage V, the voltage of half-maximal inactivation V_h, the slope factor k_h, and the fraction of noninactivating channels a_{ni}.

Toxin dissociation was assayed by measuring the degree of inactivation at 0 mV 4.5–5 ms after the start of the depolarization. For this purpose, the mean current between 4.5 and 5 ms was divided by the peak current: I_{5ms}/I_{peak}. All experiments were performed with twin pulses. In this way it was assured by the first depolarization that full recovery from slow inactivation and full toxin binding has happened
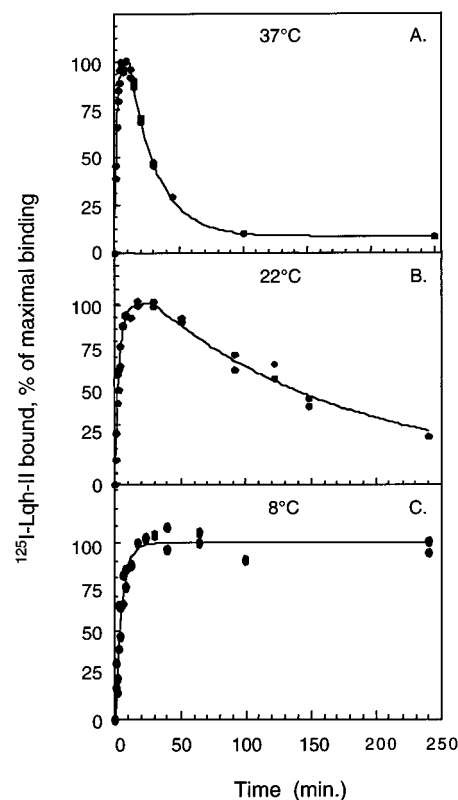

FIGURE 1: Time course of Lqh-II binding to rat brain synaptosomes at different temperatures. Rat brain synaptosomes were incubated in 200 μL of binding buffer (see Experimental Procedures) at 37 °C (panel A; 78.8 μg of protein/mL), 22 °C (panel B; 20 μg/mL), or 8 °C (panel C; 20 μg/mL). Association kinetics were measured in the presence of ^{125}I-Lqh-II at 126 pM (37 °C) or 60 pM (8 and 22 °C). Typical experiments are presented. Nonspecific binding determined in parallel experiments in the presence of 1 μM Lqh-II was time-invariant and was subtracted from the experimental points. The binding of ^{125}I-Lqh-II reached its maximum level after 5, 10, and 20 min respectively at 37, 22, and 8 °C and was stable for 5, 30, and more than 240 min before starting to decrease. Maximal binding (100%) was 0.21, 0.017, and 0.007 fmol/mg at 37, 22, and 8 °C, respectively.

before conditioning pulses were applied (for further protocol details see ref *47*).

RESULTS

Monitoring Spontaneous Depolarization of Synaptosomes. At resting membrane potential of rat brain synaptosomes (∼−55 mV with 5 mM external K^+; *30, 32, 37, 39*), classical α-toxins, such as Aah-II and Lqh-II, bind with high affinity (K_d of 0.2–0.3 nM; *27, 43*). The saturable binding of these α-toxins is reduced by ∼90% upon membrane depolarization with 90–135 mM K^+ (membrane potential of ∼0 mV; *29, 32, 33, 39, 48*). It has been demonstrated that the decrease in binding affinity in high external $[K^+]$ was due to its effect on membrane depolarization and not a direct effect on scorpion α-toxin binding, as equivalent changes in α-toxin affinity occurred when membrane potential was depolarized by various methods (*21, 30, 32, 33*). Depolarization of the membrane potential occurs spontaneously during prolonged incubation of synaptosomes in 5 mM $[K^+]$ (∼−55 mV) buffer and is monitored by the change in ^{125}I-Lqh-II binding with time (Figure 1). Specific binding of ^{125}I-Lqh-II at 5 mM $[K^+]$ reached a maximum level and then decreased at various rates, depending on the temperature. The decrease in ^{125}I-
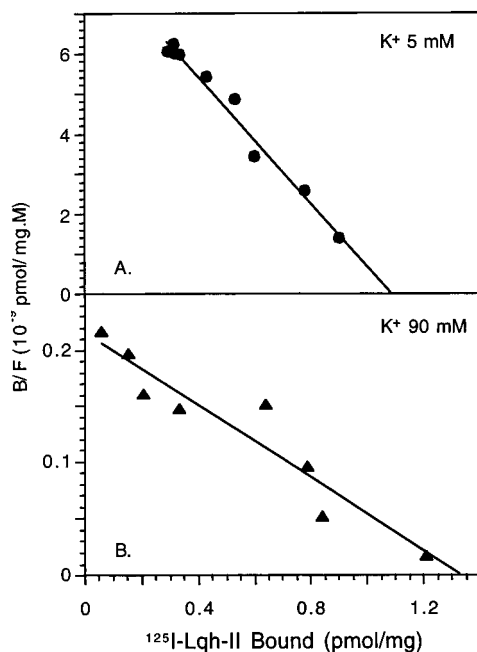
FIGURE 2: Scatchard plots of the binding of ^{125}I-Lqh-II to rat brain synaptosomes under polarized (5 mM K⁺) and depolarized (90 mM K⁺) conditions. Synaptosomes were incubated with ^{125}I-Lqh-II at 22 °C for 20 min in binding buffer containing 5 mM K⁺ (13.6 μg of protein in 1 mL reaction volume; 33 pM ^{125}I-Lqh-II) and for 60 min in 90 mM K⁺ (11.6 μg of protein in 0.2 mL reaction volume; 268 pM ^{125}I-Lqh-II), in the presence of increasing concentrations of nonlabeled Lqh-II (cold saturation), so that [choline] plus [K⁺] was 135.5 mM. Nonspecific binding, determined in the presence of 0.2 and 1 μM Lqh-II, respectively, was subtracted. The equilibrium binding parameters were calculated by the program LIGAND (see Experimental Procedures) and were as follows (mean ± SE; n = number of experiments) under polarized conditions: K_d = 0.18 ± 0.04 nM; B_{max} = 0.86 ± 0.3 pmol/mg of protein (n = 3). Under depolarized conditions: K_d = 5.85 ± 0.5 nM; B_{max} = 1.4 ± 0.2 pmol/mg (n = 4).

Lqh-II binding was attributed to the passive dissipation of the K⁺ ion gradient with time, which caused progressive depolarization of the membrane potential. The potential was stable for 10 min at 37 °C (Figure 1A), for 40 min at 22 °C (Figure 1B), and for more than 4 h at 8 °C (Figure 1C). The short-lived steady-state polarized membrane potential at 37 °C as well as the low specific binding at 8 °C (approximately 40% of that at 22 °C; see Figure 1 caption) posed difficulties in performing a detailed kinetic analysis of Lqh-II binding. Thus, all subsequent studies were performed at 22 °C, which allowed the appropriate setting for precise binding analyses under both kinetic and equilibrium conditions at polarized membrane potential at steady state. In addition, this temperature allowed a more direct comparison of the binding data with results obtained from electrophysiological experiments.

Affinity of ^{125}I-Lqh-II for Polarized and Depolarized Rat Brain Synaptosomes at Steady State. The change in equilibrium dissociation constant (K_d) of ^{125}I-Lqh-II binding under polarized (5 mM K⁺) and depolarized (90 mM K⁺) conditions was determined by Scatchard analysis of saturation binding curves of Lqh-II (Figure 2). The concentration of ^{125}I-Lqh-II and receptor sites (membrane protein) at equilibrium was adjusted to the different apparent affinity values to keep the change in free ^{125}I-Lqh-II under 10% (see Figure 2 caption; *45*). Under optimal conditions, the specific binding
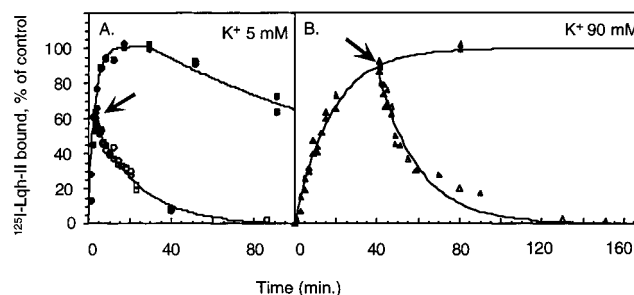

FIGURE 3: Kinetics of ^{125}I-Lqh-II binding to polarized and depolarized membranes. Rat brain synaptosomes were incubated at 22 °C (in 200 μL) in the presence of (A) 5 mM K⁺ and 84 pM^{125}I-Lqh-II (35 μg/mL protein) and (B) 90 mM K⁺ and 220 pM ^{125}I-Lqh-II (73 μg/mL protein), for various periods of time. Nonspecific binding, determined in parallel in the presence of 200 nM or 1 μM Lqh-II, respectively, was time-invariant and subtracted from the experimental points. Dissociation was initiated by addition of (arrows) 200 nM or 1 μM nonlabeled toxin after 3 or 60 min of association at polarized and depolarized conditions, respectively. At polarized condition (A), 80% of the dissociation of the bound toxin was achieved before the occurrence of spontaneous depolarization of the membranes (see text).

was 95% and 70% of the total binding in 5 and 90 mM K⁺, respectively, which enabled an accurate estimation of the binding parameters under steady-state conditions. The Scatchard analyses indicated a single receptor binding site, as was previously described (*32, 33*). The apparent binding affinity of Lqh-II dropped 33-fold from polarized (5 mM K⁺; K_d = 0.18 ± 0.04 nM, n = 3; mean ± SE, n = number of experiments) to depolarized (90 mM K⁺; K_d = 5.85 ± 0.5, n = 4) conditions and was accompanied by a 1.6-fold increase in receptor site capacity (B_{max} = 0.86 ± 0.3 pmol/ mg of protein and n = 3 for polarized membranes; B_{max} = 1.4 ± 0.2 pmol/mg of protein and n = 4 for depolarized membranes) (Figure 2).

Association and Dissociation Kinetics of ^{125}I-Lqh-II Binding. Analysis of the binding curves in Figures 1 and 2 indicated the significance of measurements at steady-state polarized conditions for the precise determination of binding parameters. Hence, ^{125}I-Lqh-II dissociation at polarized membrane potential was induced by addition of excess Lqh-II (200 nM, Figure 3A, arrow) after 3 min of association. This ensured stable membrane potential throughout the dissociation measurements as indicated by the increase in ^{125}I-Lqh-II binding in the control (Figure 3A). Approximately 80% of the bound ^{125}I-Lqh-II dissociated before spontaneous depolarization of the membrane could be detected, as was shown by the gradual decrease in binding after 30 min of incubation in the control (Figure 3A). The calculated association rate constant, k_{on}, of Lqh-II at polarized membrane conditions was (12.0 ± 4.0) × 10⁶ M⁻¹ s⁻¹ (n = 6), and that of the dissociation rate, k_{off}, was (0.82 ± 0.06) × 10⁻³ s⁻¹ (n = 3). The corresponding K_d, calculated from the kinetic constants, was 68.3 pM, which was in good accordance with the value obtained at equilibrium (Figure 2). Kinetics of ^{125}I-Lqh-II binding in depolarized synaptosomes (90 mM K⁺) was easier to measure. Dissociation was induced by 1 μM Lqh-II (arrow, Figure 3B), and the calculated binding parameters were k_{on} = (0.25 ± 0.03) × 10⁶ M⁻¹ s⁻¹ (n = 4) and k_{off} = (1.12 ± 0.08) × 10⁻³ s⁻¹ (n = 3). The corresponding calculated K_d was 4.48 nM, which was in good agreement with the equilibrium measurements (Figure 2).
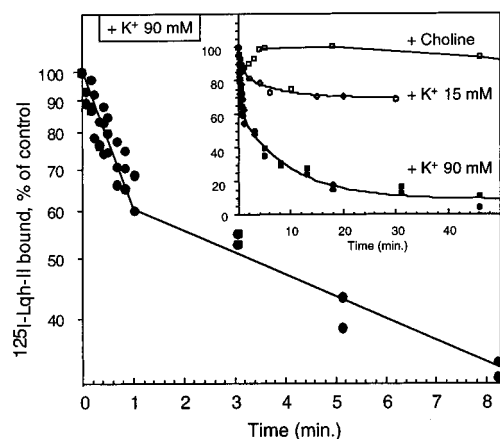
FIGURE 4: Effects of fast depolarization of synaptosomes on the binding of ^{125}I-Lqh-II. Synaptosomes (90 μg/mL protein) were incubated at 22 °C for 20 min in a 5 mM K$^+$ binding buffer (-55 mV membrane potential) with 120 pM ^{125}I-Lqh-II. Then, one volume of 180 mM K$^+$ (90 mM K$^+$ final concentration; main panel and inset) or 1 volume of 180 mM choline (control; inset) binding buffer, each containing 120 pM ^{125}I-Lqh-II, were added and the evolution of the binding was monitored at different time periods. In some experiments, partial depolarization was obtained by addition of 0.058 volume of 180 mM K$^+$ binding buffer (15 mM K$^+$ final concentration) containing 120 pM of ^{125}I-Lqh-II (inset). Nonspecific binding, determined in parallel experiments in the presence of 1 μM Lqh-II, was time-invariant and was subtracted from the experimental points. The additions induced a complete depolarization (0 mV, 90 mM K$^+$), no change in membrane potential (control, choline buffer), or a partial depolarization (-30 mV; 15 mM K$^+$) and resulted in a 2-fold dilution of receptor sites. During the first 60 s after each addition the binding was measured in triplicate at 10 s intervals (see Experimental Procedures). Main panel presents enlargement of the binding curve of the first 8 min after depolarization to 0 mV (90 mM K$^+$), drawn on a semilog scale, which revealed the two-slopes fit of the binding results. See text for details.

Unexpectedly, the difference between the dissociation rates under polarized and depolarized conditions could not explain the drop in affinity. This result implied that the membrane potential per se had nearly no effect on the dissociation rate of the complex under our binding conditions. More unexpected was the finding that the association rate constant decreased 48-fold at depolarized membrane potential, which could account for the change in K_d values at polarized and depolarized synaptosomes.

Effect of Instantaneous Depolarization on the Binding of ^{125}*I-Lqh-II.* The increase in dissociation rate of scorpion α-toxin binding due to membrane depolarization has been inferred from electrophysiological experiments in which it was shown that the toxin effect on fast inactivation can be diminished by depolarizing prepulses (e.g., *21* and *22*). To mimic a fast membrane depolarization in our binding studies, we quickly elevated [K$^+$] to 90 mM with no change in the free ^{125}I-Lqh-II toxin concentration. Synaptosomes were allowed to bind ^{125}I-Lqh-II at polarized conditions (5 mM K$^+$) for 20 min; subsequently, the membranes were instantaneously depolarized by 1:1 (v/v) addition of 180 mM K$^+$ (90 mM K$^+$ final) containing identical ^{125}I-Lqh-II concentration (120 pM; see Figure 4). The small change in osmolarity of the binding buffer (from 300 to 330 mOsm) had no effect on ^{125}I-Lqh-II binding (data not shown). In parallel, identical addition of choline or a lower [K$^+$] (135 mM choline or 15 mM K$^+$ final concentrations) were performed in control

experiments (Figure 4, inset). The binding of ^{125}I-Lqh-II remained practically constant for at least 40 min after addition of choline, except for a ~10% initial transient decrease during the first 2–4 min, indicating that the 2-fold dilution of receptor sites per se had no significant effect on the toxin–receptor complex (Figure 4, inset). In contrast, dilution by high [K$^+$] (90 mM final concentration) induced an immediate 50% drop in bound toxin during the first minute (Figure 4, inset). Statistical analysis of the data and a semilogarithmic presentation of the drop in binding yielded two slopes in the binding curve ($p < 0.01$, by LIGAND kinetic analysis, Figure 4 main panel). The first slope corresponded to the first minute postdepolarization, during which the saturable binding decreased by 35–40%, with a time constant of 15.8 s ($n = 3$). Assuming no significant association of the toxin during the first 60 s, the calculated dissociation rate constant (k_{off}) was $(44 \pm 14) \times 10^{-3}$ s^{-1} (Table 1). This calculation is acceptable since the time constant of association at depolarized membranes is 18 min, and less than 10% of the toxin is able to rebind during the first minute, which is within the experimental error of the k_{off} calculation. The second slope (starting after 60 s), with a time constant of 533 $\pm$ 280 s ($n = 3$), revealed a 34.5-fold slower decrease in binding than that of the first slope. The calculated off rate, $k_{off} = (1.3 \pm 0.7) \times 10^{-3}$ s^{-1}, was very similar to that obtained with depolarized synaptosomes at steady state (Figure 3, Table 1). An intermediate depolarization by 15 mM K$^+$ caused a decrease in ^{125}I-Lqh-II binding also typified by two slopes. The first slope had a time constant of 33 s and represented only 15% decrease in binding, whereas the second slope displayed a 10-fold slower decrease in bound toxin, with a time constant of 330 s (off rate of 2.1×10^{-3} s^{-1}), and reached 70% of the initial binding at steady state. The second slope was in concert with the dissociation rate constant measured under steady-state depolarization (Figure 3). The slower phase of toxin unbinding (Figure 4) reaches a new equilibrium (10% and 70% of the initial value of bound toxin, at 90 or 15 mM K$^+$, respectively) that can be calculated from the concentration of the bound toxin complex (RL) at each membrane potential, and the K_d, by the equation $RL = [R][L]/K_d$. The initial RL value was obtained from Lqh-II binding to polarized synaptosomes (low K_d and high RL; Table 1). The profound increase of K_d upon fast depolarization by 90 mM K$^+$ explains the low RL value obtained (10% of the initial level; Figure 4). The time required to achieve a new equilibrium is a function of the k_{off}, which is nearly independent of membrane potential, and of the slow k_{on} under depolarized conditions (Figure 3, Table 1). Indeed, the close resemblance between the second apparent off rate (after more than 1 min from fast depolarization, Figure 4) and the k_{off} value obtained at steady state (Table 1) suggest that the new equilibrium represents binding to equivalent channel states, presumably the slow-inactivated states. This is supported by the off rate value calculated under partially depolarized conditions (15 mM K$^+$, $k_{off} = 2.1 \times 10^{-3}$ s^{-1}), which resembles that measured under steady-state conditions.

Effect of Lqh-II on Fast and Slow Inactivation of rBII Sodium Channels. Upon heterologous expression in HEK293 or CHO cells, the function of rBII channels was assayed with patch clamp methods. As shown previously, application of Lqh-II to the extracellular side of the cell substantially slows down the fast inactivation of rBII sodium channels (Figure

Table 1: Binding Parameters of Lqh-II to Polarized and Depolarized Rat Brain Synaptosomes under Steady-State Conditions and Following Induced Fast Depolarization[a]

| binding parameter | synaptosomes at steady-state conditions | | fast depolarization (by 90 mM K$^+$) applied on the toxin−receptor complex | |
	polarized (−55 mV; 5 mM K$^+$)	depolarized (0 mV; 90 mM K$^+$)	fast component	slow component
K_d (nM)	0.18 ± 0.04 ($n = 3$)	5.85 ± 0.5 ($n = 4$)		
B_{max} (pmol/mg)	0.86 ± 0.3 ($n = 3$)	1.4 ± 0.2 ($n = 4$)		
k_{on} (10^6 M^{-1} s^{-1})	12.0 ± 4 ($n = 6$)	0.25 ± 0.03 ($n = 4$)		
k_{off} (10^{-3} s^{-1})	0.82 ± 0.06 ($n = 3$)	1.12 ± 0.08 ($n = 3$)	44 ± 14 ($n = 3$)	1.3 ± 0.7 ($n = 3$)

[a] Values are from Figures 2−4, presented as mean ± SEM, n = number of independent experiments.
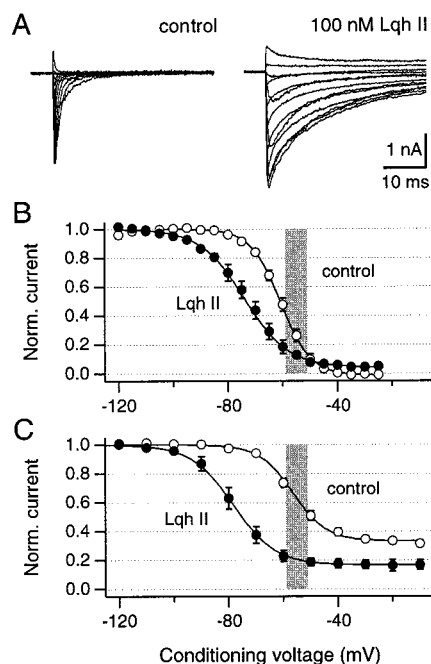

FIGURE 5: Steady-state fast and slow inactivation of rBII sodium channels, expressed in HEK293 cells. (A) Current traces in response to depolarizations from −60 to +60 mV in steps of 10 mV in the absence (left) and presence (right) of 100 nM Lqh-II. Currents were low-pass-filtered at 5 kHz. (B) Voltage dependence of steady-state fast inactivation of rBII channels without (control) and after application of 100 nM Lqh-II. The current was measured at −20 mV, and the prepulses to the indicated voltages lasted 500 ms. (C) Voltage dependence of steady-state slow inactivation. In this cases prepulses were applied for 60 s. Pulses of 50 ms to −140 mV before the test depolarization to 0 mV ensured recovery from fast inactivation. The holding voltage of all experiments was −120 mV; the repetition interval for fast inactivation was 10 s. Slow inactivation was measured with twin pulses (see text) after removal of slow inactivation with 40-s pulses to −140 mV. The error bars indicate SEM values for $n = 5$.

5A) and shifts the activation by about −10 mV (*48*). Here we were interested in the degree of channel inactivation obtained after conditioning pulses of different lengths. Typically, voltage dependence of fast Na$^+$ channel inactivation is assayed by conditioning pulses of 500 ms duration. As shown in Figure 5B, such a protocol results in a steady-state inactivation, fit by a Boltzmann function with the half-maximal inhibition at −61 ± 1 mV and a slope factor of 5.5 ± 0.3 mV. After application of 100 nM Lqh-II, fast inactivation starts at more negative voltages and exhibits a

smaller voltage dependence: $V_h = -74 \pm 1$ mV; $k_h = 8.1 \pm 0.4$ mV ($n = 5$).

Slow inactivation was assayed by twin pulses to 0 mV. After the first pulse, conditioning pulses of 60 s duration were applied. To recover the channels from fast inactivation, 50-ms pulses to −140 mV were applied after the conditioning pulse and before the test pulse, during which the noninactivating currents were measured. The resulting currents were normalized to the current during the first depolarization in order to eliminate slow drift phenomena. Unlike fast inactivation, slow inactivation is not complete at high voltages. The fit to the control data shown in Figure 5C yielded $V_s = -56 \pm 1$ mV, $k_s = 6.2 \pm 0.5$ mV, and a noninactivating component of 33% ± 1%. After application of 100 nM Lqh-II, slow inactivation was substantially shifted to more negative voltages: $V_h = -78 \pm 2$ mV and $k_h = 7.7 \pm 0.8$ mV. In addition, the noninactivating component was reduced to 17% ± 2%. Thus, although Lqh-II substantially removes fast inactivation of rBII channels, it causes a marked increase in steady-state fast and slow inactivation. At a membrane potential of −70 mV for 60 s, the toxin-induced decrease in peak current can be as large as 60%. The shaded areas in Figure 5B,C indicate the expected voltage of resting, polarized synaptosomes; it is clearly seen that rBII channels in synaptosomes, in particular in the presence of Lqh-II, will have entered both fast- and slow-inactivated states to a substantial degree.

To estimate the voltage dependence of toxin dissociation in the presence of 100 nM Lqh-II, the degree of fast inactivation, used as an indicator for toxin binding, after depolarizing pulses of varying duration was measured by the current after 5 ms relative to the peak current (not shown). Toxin dissociation was observed to proceed with a single-exponential time course. The resulting time constants are shown in Figure 6 as filled symbols.

DISCUSSION

Sodium Channel States under Polarized and Depolarized Conditions. The Na$^+$ channels in rat brain synaptosomes are about 80% type II (rBII) and approximately 20% type I (rBI) (*49*). The synaptosome membrane voltage can be modulated in the range of roughly −55 to 0 mV. Our results for rBII channels expressed in mammalian cells show that these channels populate a mixture of states at −55 mV. About 10% of the channels can be fully activated by depolarization
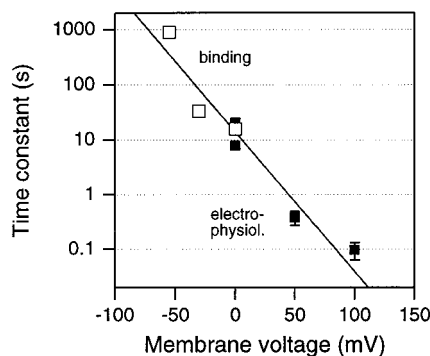
FIGURE 6: Time constants of Lqh-II unbinding as a function of the membrane potential. Data from electrophysiological measurements are presented (on a semilog scale) together with results from the binding studies. The closed symbols represent the time constants of Lqh-II unbinding at different membrane potentials measured electrophysiologically on rBII sodium channels expressed in mammalian cells. The open symbols represent time constants of Lqh-II unbinding of rat brain synaptosomes. Changes in membrane potential of synaptosomes were obtained by increasing external K^+ concentrations (5, 15, and 90 mM) to obtain -55, -30, and 0 mV, respectively. The time constants of Lqh-II unbinding at -30 and 0 mV are from Figure 4. The time constant at -55 mV was calculated from the k_{off} obtained in Figure 3. The error bars for the electrophysiological data represent the errors obtained from fitting single-exponential functions to dissociation data. Notably, the time constants of Lqh-II unbinding at the various membrane potentials of synaptosomes fit remarkably well to a line, which could be extrapolated from the electrophysiological measurements. The straight line indicates an exponential fit yielding a slope of (17 mV/e)-fold change in the time constant.

to -55 mV (48), but the probability of the individual activating units, i.e., the S4 segments, being in the activated position at -55 mV is substantially greater. However, only a small fraction will actually be open at a holding voltage of -55 mV, because most channels will be inactivated. Indeed, the data in Figure 5 show that about 75% of the channels are fast-inactivated and about 40% are slow-inactivated. In the presence of a saturating concentration (100 nM) of Lqh-II, inactivation is even more prevalent: about 80% of the channels are fast- and slow-inactivated. Therefore, at -55 mV, rBII Na^+ channels in rat synaptosomes are expected to populate a complex mixture of states: the S4 segments are about half-activated and the channels have substantially entered fast- and slow-inactivated states.

Rapid depolarization, as induced in the experiments shown in Figure 4, will result in an alteration of the state population. Activation of the S4 segments will reach almost saturation and the extent of fast and slow inactivation will only increase slightly in absolute terms (about an additional 10%). In relative terms, however, fast and slow inactivation increase substantially, i.e., from the noninactivated channels at -55 mV, almost 100% will undergo fast and 50% will undergo slow inactivation.

These data show, at least for the fraction of rBII channels in synaptosomes, that toxin-binding studies to Na^+ channels will mostly report on electrically silent conformational changes because most of the channels are not accessible by electrophysiological methods at the voltages under consideration. Rat brain synaptosomes, however, contain about 20% rBI channels, which according to Smith and Goldin (50) are available for opening at -55 mV, when assayed in *Xenopus* oocytes with coexpression of $\beta1$ and $\beta2$ subunits. Thus, the

fraction of activable channels may indeed be greater than estimated from the electrophysiological assessment of rBII channels alone.

Capacity of Lqh-II Binding Sites on Polarized and Depolarized Synaptosomes. We found that the capacity of Lqh-II to bind polarized synaptosomes (0.86 pmol/mg) represents 60% of the capacity on depolarized synaptosomes (1.4 pmol/mg). This result suggests that 60% of the channels at -55 mV are in states presenting a high-affinity binding site for Lqh-II, and the rest are in other states, which correspond to the low-affinity site. The reason, on polarized synaptosomes, we did not detect the low-affinity site is due to the low concentrations of ^{125}I-Lqh-II (compared to its K_d) used in the binding studies (Figures 1 and 2). Such low toxin concentration prevented detection of low-affinity binding sites in polarized synaptosomes, because only 20% and 0.3% of the high- and low-affinity sites, respectively, were occupied. In contrast, in depolarized synaptosomes, close to 100% of the Na^+ channels occupy states presenting a more uniform, low-affinity site to the toxin, and maximal binding capacity was obtained (Figure 2). This conclusion is supported by the data obtained with the binding of a spider toxin, δ-atracotoxin, and allosteric modulation of site 3 toxin binding by alkaloid sodium channel activators (unpublished results). The direct designation, however, of channel states followed in the binding studies is not straightforward. Considering the state distribution obtained for rBII channels in HEK293 cells, this likely reflects a transition from deactivated to activated S4 segments. However, it cannot be excluded that it represents a transition of the slow inactivation gate, which is also about half-activated at -55 mV. More insight may be gained by considering the kinetics and voltage dependence underlying such a transition.

Channel State Transition between High- and Low-Affinity Sites. Electrophysiological studies suggested that binding of α-toxins slow the transition from open to fast-inactivated channel states and that the decline in toxin binding affinity at depolarized conditions resulted from a strong increase in the off rate (21, 30, 31, 35, 36, 51). However, transitions that occur between different inactivated states are electrically silent and therefore are difficult to study.

To analyze the direct effect of fast depolarization on binding of α-toxins, we have pursued the change in Lqh-II binding after instantaneous depolarization of membranes, which were preequilibrated with toxin at resting membrane potential. Induction of fast depolarization was achieved by increasing the K^+ concentration while maintaining a constant concentration of free ^{125}I-Lqh-II in order to prevent toxin dissociation by dilution (Figure 4), which mimicked the electrophysiological experiments in the presence of α-toxins (21). The fast toxin unbinding rate in the electrophysiological approach was inferred from the loss of toxin effect on current inactivation and was attributed to the transition from closed to fast-inactivated channel states through the open state (21, 36). Judicious analysis of ^{125}I-Lqh-II unbinding after fast depolarization provided an off-rate value of 44×10^{-3} s^{-1} for the fast component (Figure 4 and Table 1), which is strikingly similar to that obtained for Lqh-II in electrophysiological studies on rBII Na^+ channels, expressed in mammalian cells. This similarity can be demonstrated by plotting the time constants of Lqh-II unbinding at different membrane potentials (filled symbols in Figure 6) together with those

obtained in the Lqh-II binding experiments (open symbols in Figure 6). The data fit in Figure 6 according to a single-exponential function to the combined data shows that the time constant of Lqh-II dissociation from rBII/rat synaptosome channels has a voltage dependence equivalent to (17 mV/e)-fold change.

These equivalent off rates suggest a transition into identical channel states during the first phase after fast depolarization of synaptosomes (Figure 4) and depolarization under voltage-clamp conditions. The high off rate is likely to represent a fast conformational change at the toxin receptor site, which destabilizes the toxin−receptor complex and leads to toxin expulsion. This change could occur during the rapid transition from the closed to the activated and finally the fast-inactivated state, as was suggested in the electrophysiological studies (*21*, *36*). Owing to the similarity in rate and voltage dependence of this component determined in electrophysiological and binding assays, it can be concluded that it is not associated with slow-inactivated channel states, because they would not be detected with the electrophysiological protocols employed.

The second, slow unbinding component (Figure 4) provides an equivalent off rate to that measured in depolarized synaptosomes at steady state (Figure 3 and Table 1). This similarity suggests that the unbinding during this second slow phase occur from channels in slow-inactivated states. This interpretation is supported by the kinetics (seconds to minutes) of entering into the slow-inactivated state of Na⁺ channels in various depolarized neural preparations (*12*, *52−56*). Moreover, no marked slow component of toxin dissociation is observed in electrophysiological experiments, suggesting that this component, measured in binding experiments, represents electrically silent channel states. Such states could become more populated after depolarization, leading to slow unbinding of the toxin. Slow inactivation has been described as an absorbing state, which is effectively sequential to channel activation (*55−57*). The observation that only about 50% of the bound Lqh-II at resting membrane potential is expelled by fast depolarization (Figure 4) may indicate that about half the channels with bound toxin undergo a direct transition to the slow-inactivated state. In addition, the strength of toxin binding to such states may have a small intrinsic voltage dependence, which may contribute to the small change in toxin k_{off} upon depolarization (Table 1).

The rapid and extended depolarization of synaptosomes may induce slow inactivation of the Na⁺ channels, leading to conformational changes of these proteins with time constants in the order of several seconds to minutes (see Figure 4). In addition, application of the toxins will enhance slow inactivation (see Figure 5) and therefore will alter the equilibrium of normal and slow-inactivated channel states, which may have different affinities for the toxins. The voltage-dependent decrease in k_{on} suggests a creation of a steric hindrance and/or charge alteration at the vicinity of receptor site 3, which reduce toxin association to the slow-inactivated state. The smaller difference in association rates of the structurally different δ-atracotoxin to receptor site 3 under polarized and depolarized conditions further supports this notion (unpublished results).

CONCLUDING REMARKS

Our results reveal that it is the association and not the dissociation rate, observed in α-toxin binding, which is voltage-dependent. The association rate is substantially reduced in depolarized membranes, linked to the slow-inactivated state. A second distinct mechanism exists that causes a voltage-dependent expulsion of the bound toxin. It is suggested that rapid membrane depolarization induces a fast transition to channel states that are responsible for the destabilization of the bound α-toxin and its subsequent expulsion from the receptor site. The voltage dependence of this process is similar to that observed in electrophysiological experiments (Figure 6 and, e.g., refs *21* and *36*), suggesting that it reports on structural changes of electrical visible channel states, i.e., transitions of non-slow-inactivated channels. The altered association rate and the slow dissociation may report on channel states that are not accessed by electrophysiological methods, i.e., transitions to or among slow-inactivated channel states, which are prevalent at the relatively low membrane voltages of rat brain synaptosomes.

This study paves the way to further analysis of the putative effects of α-toxins on channel entrance to and recovery from the slow-inactivated state, which may shed light on structural elements involved in modulation of receptor site 3.

REFERENCES

1. Noda, M., Ikeda, T., Suzuki, H., Takeshima, H., Takahashi, T., Kuno, M., and Numa, S. (1986) *Nature 320*, 188−192.
2. Stühmer, W., Conti, F., Suzuki, H., Wang, X., Noda, M., Yahagi, N., Kubo, H., and Numa, S. (1989) *Nature 339*, 597−603.
3. Aggarwal, S. K., and MacKinnon, R. (1996) *Neuron 16*, 1169−1177.
4. Armstrong, C. M. (1981) *Physiol. Rev. 61*, 644−682.
5. Yang, N., George, A. L., Jr, and Horn, R. (1996) *Neuron 16*, 113−122.
6. Cha, A., Ruben, P. C., George, A. L., Jr., Fujimoto, E., and Bezanilla, F. (1999) *Neuron 22*, 73−87.
7. Chahine, M., George, A., Jr., Zhou, M., Ji, S., Sun, W., Barchi, R. L., and Horn, R. (1994) *Neuron 12*, 281−294.
8. Chen, L. Q., Santarelli, V., Horn, R., and Kallen. R. G. (1996) *J. Gen. Physiol. 108*, 549−556.
9. McPhee, J. C., Ragsdale, D. S., Scheuer, T., and Catterall, W. A. (1994) *Proc. Natl. Acad. Sci. U.S.A. 91*, 12346−12350.
10. McPhee, J. C., Ragsdale, D. S., Scheuer, T., and Catterall, W. A. (1995) *J. Biol. Chem. 270*, 12025−12034.
11. McPhee, J. C., Ragsdale, D. S., Scheuer, T., and Catterall, W. A. (1998) *J. Biol. Chem. 273*, 1121−1129.
12. Kontis, K. J., and Goldin, A. L. (1997) *J. Gen. Physiol. 110*, 403−413.
13. Vassilev, P., Scheuer, T., and Catterall, W. A. (1988) *Science 241*, 1658−1661.
14. West, J. W., Patton, D. E., Scheuer, T., Wang, Y., Goldin, A. L., and Catterall, W. A. (1992) *Proc. Natl. Acad. Sci. U.S.A. 89*, 10910−10914.
15. Catterall, W. A. (1992) *Physiol. Rev. 72* (*Suppl.*), S15−S48.
16. Gordon, D. (1997) in *Toxins and Signal Transduction* (Lazarovici, P., and Gutman, Y., Eds.) pp 119−149, Harwood Press, Amsterdam.
17. Gordon, D. (1997) *Invertebr. Neurosci. 3*, 103−116.
18. Martin-Eauclaire, M. F., and Couraud, F. (1995) in *Handbook Neurotoxicology* (Chang, L. W., and Dyer, R. S., Eds.) pp 683−716, Marcel Dekker, New York.
19. Thomsen, W. J., and Catterall, W. A. (1989) *Proc. Natl. Acad. Sci. U.S.A. 86*, 10161−10165.
20. Tejedor, F., and Catterall, W. A. (1990) *Cell. Mol. Neurobiol. 10*, 257−265.

21. Rogers, J. C., Qu, Y., Tanada, T. N., Scheuer, T., and Catterall, W. A. (1996) *J. Biol. Chem. 271*, 15950−15962.

22. Benzinger, G. R., Kyle, J. W., Blumenthal, K. M., and Hanck, D. A. (1998) *J. Biol. Chem. 273*, 80−84.

23. Ma, Z., Tang, L., Lu, S., Kong, J., Gordon, D., and Kallen, R. G. (2000) *Biophys. J. 78*, A1011.

24. Zilberberg, N., Froy, O., Loret, E., Cestèle, S., Arad, D., Gordon, D., and Gurevitz, M. (1997) *J. Biol. Chem. 272*, 14810−14816.

25. Gurevitz, M., Gordon, D., Ben-Natan, S., Turkov, M. and Froy, O. (2001) *FASEB J. 15*, 1201−1205.

26. Catterall, W. A. (1977) *J. Biol. Chem. 252*, 8669−8676.

27. Cestèle, S., Ben Khalifa, R., Pelhate, M., Rochat, H., and Gordon, D. (1995) *J. Biol. Chem. 270*, 15153−15161.

28. Cestèle, S., Sampieri, F., Rochat, H., and Gordon, D. (1996) *J. Biol. Chem. 271*, 18329−18332.

29. Cestèle, S., and Gordon, D. (1998) *J. Neurochem. 70*, 1217−1226.

30. Catterall, W. A., Ray, R., and Morrow, C. S. (1976) *Proc. Natl. Acad. Sci. U.S.A. 73*, 2682−2686.

31. Catterall, W. A. (1977) *J. Biol. Chem. 252*, 8660−8668.

32. Ray, R., Morrow, C. S., and Catterall, W. A. (1978) *J. Biol. Chem. 253*, 7307−7313.

33. Jover, E., Martin-Moutot, N., Couraud, F., and Rochat, H. (1980) *Biochemistry 19*, 463−467.

34. Mozhayeva, G. N., Naumov, A. P., Nosyreva, E. D., and Grishin, E. V. (1980) *Biochim. Biophys. Acta. 597*, 587−602.

35. Strichartz, G. R., and Wang, G. K. (1986) *J. Gen. Physiol. 88*, 413−435.

36. Chen, H., Gordon, D., and Heinemann, S. H. (2000) *Pflügers Arch. 439*, 423−432.

37. Catterall, W. A., Morrow, C. S., and Hartshorne, R. P. (1979) *J. Biol. Chem. 254*, 11379−11387.

38. Sautière, P., Cestèle, S., Kopeyan, C., Martinage, A., Drobecq, H., Doljansky, Y., and Gordon, D. (1998) *Toxicon 36*, 1141−1154.

39. Blaustein, M. P., and Goldring, J. M. (1975) *J. Physiol. 247*, 589−615.

40. Tamkun, M. M., and Catterall, W. A. (1981) *Mol. Pharmcol. 19*, 78−86.

41. Sharkey, R. G., Jover, E., Couraud, F., Baden, D. G., and Catterall, W. A. (1987) *Mol. Pharmacol. 31*, 273−278.

42. Kanner, B. J. (1978) *Biochemistry 17*, 1207−1211.

43. Gilles, N., Blanchet, C., Shichor, I., Zaninetti, M., Lotan, I., Bertrand, D., and Gordon, D. (1999) *J. Neurosci. 19*, 8730−8739.

44. Gilles, N., Krimm, I., Bouet, F., Froy, O., Gurevitz, M., Lancelin, J.-M., and Gordon, D. (2000) *J. Neurochem. 75*, 1735−1745.

45. Weiland, G. A., and Molinoff, P. B. (1981) *Life Sci. 29*, 313−330.

46. Jurman, M. E., Boland, L. M., Liu, Y., and Yellen, G. (1994) *Biotechniques 17*, 876−881.

47. Chen, H., and Heinemann S. H. (2001) *J. Gen. Physiol. 117*, 505−518.

48. Gilles, N., Chen, H., Wilson, H., Le Gall, F., Montoya, G., Molgo, J., Schönherr, R., Nicholson, G., Heinemann, S. H., and Gordon, D. (2000) *Eur. J. Neurosci. 12*, 2823−2832.

49. Gordon, D., Merrick, D., Auld, V., Dunn, R., Goldin, A. L., Davidson, N., and Catterall, W. A. (1987) *Proc. Natl. Acad. Sci. U.S.A. 84*, 8682−8686.

50. Smith, R. D., and Goldin, A. L. (1998) *J. Neurosci. 18*, 811−820.

51. Sheets, M. F., Kyle, J. W., Kallen, R. G., and Hanck, D. A. (1999) *Biophys. J. 77*, 747−757.

52. Ruben, P. C., Starkus, J. G., and Rayner, M. D. (1990) *Biophys. J. 58*, 1169−1181.

53. Ruben, P. C., Starkus, J. G., and Rayner, M. D. (1992) *Biophys. J. 61*, 941−955.

54. Rudy, B. (1978) *J. Physiol. (London) 283*, 1−21.

55. Adelman, W. J., Jr., and Palti, Y. (1969) *J. Gen. Physiol. 54*, 589−606.

56. Rudy, B. (1981) *J. Physiol. (London) 312*, 531−549.

57. Vedantham, V., and Cannon, S. C. (1998) *J. Gen. Physiol. 111*, 83−93.

58. Featherstone, D. E., Richmond, J. E., and Ruben, P. C. (1996) *Biophys. J. 71*, 3098−3109.

59. Richmond, J. E., Featherstone, D. E., Hartmann, H. A., and Ruben, P. C. (1998) *Biophys. J. 74*, 2945−2952.